

Organic & Biomolecular Chemistry

www.rsc.org/obc

Volume 11 | Number 28 | 28 July 2013 | Pages 4561–4728



ISSN 1477-0520

RSC Publishing

PAPER

Pall Thordarson *et al.*

Optimising the synthesis, polymer membrane encapsulation and photoreduction performance of Ru(II)- and Ir(III)-bis(terpyridine) cytochrome c bioconjugates

Optimising the synthesis, polymer membrane encapsulation and photoreduction performance of Ru(II)- and Ir(III)-bis(terpyridine) cytochrome *c* bioconjugates†

Cite this: *Org. Biomol. Chem.*, 2013, **11**, 4602

David Hvasanov,^a Alexander F. Mason,^a Daniel C. Goldstein,^a Mohan Bhadbhade^b and Pall Thordarson^{*a}

Ruthenium(II) and iridium(III) bis(terpyridine) complexes were prepared with maleimide functionalities in order to site-specifically modify yeast iso-1 cytochrome *c* possessing a single cysteine residue available for modification (CYS102). Single X-ray crystal structures were solved for aniline and maleimide Ru(II) **3** and Ru(II) **4**, respectively, providing detailed structural detail of the complexes. Light-activated bioconjugates prepared from Ru(II) **4** in the presence of tris(2-carboxyethyl)-phosphine (TCEP) significantly improved yields from 6% to 27%. Photoinduced electron transfer studies of Ru(II)-cyt *c* in bulk solution and polymer membrane encapsulated specimens were performed using EDTA as a sacrificial electron donor. It was found that membrane encapsulation of Ru(II)-cyt *c* in PS_{140-b}-PAA₄₈ resulted in a quantum efficiency of $1.1 \pm 0.3 \times 10^{-3}$, which was a two-fold increase relative to the bulk. Moreover, Ir(III)-cyt *c* bioconjugates showed a quantum efficiency of $3.8 \pm 1.9 \times 10^{-1}$, equivalent to a ~640-fold increase relative to bulk Ru(II)-cyt *c*.

Received 28th March 2013,
Accepted 17th May 2013

DOI: 10.1039/c3ob40620b

www.rsc.org/obc

Introduction

Scientists have endeavoured to understand and exploit the modification of proteins by introducing synthetic ligands in order to enhance or introduce novel functionalities in the field of bioconjugation chemistry.¹ This has led to the development of biotechnological, biomedical and pharmaceutical industry related devices such as biosensors,² bioelectronics,³ biofuel cells⁴ and bioconjugated therapeutic proteins/drugs.⁵

In our group, we have studied light-activated bioconjugates based on redox enzymes as potential building blocks for applications ranging from hybrid solar-biofuel cells to biosensors and light-driven nanoreactors. In making these bioconjugates we are guided by three design principles: (i) the bioconjugate synthesis should be specific but straightforward using readily

available but important proteins, (ii) the excitation wavelength of the chromophores used should be easily tuneable and (iii) the bioconjugates should be readily incorporated in membranes allowing us to mimic Nature's ability to compartmentalise protein-based processes. To this end, we have mainly focused on systems based on the readily available redox enzyme iso-1 cytochrome *c* (cyt *c*) derived from *Saccharomyces cerevisiae* which is then activated by light *via* room temperature photoinduced electron transfer.^{6,7}

The light-harvesting component using tris(bipyridine)ruthenium(II) metal complexes with cytochrome *c* have been extensively studied due to their long fluorescent lifetimes and high quantum yields.^{8–10} However, in recent decades, metal complexes based on ruthenium(II) or iridium(III) bis(terpyridine) complexes have been receiving considerable attention due to their interesting photophysical, electrochemical and photochemical properties.¹¹ Moreover, bis(terpyridine) complexes are synthetically straightforward as the use of 4'-functionalised ligands avoids complications in chirality and allows simplified synthesis of heteroleptic complexes. This has already allowed us to synthesise several bis(terpyridine)ruthenium(II) complexes and bis(terpyridine)iridium(III)¹² complexes that can be excited at around 480 nm and 370 nm, respectively.

Electron transfer studies involving cytochrome *c* have been reported in literature, predominantly using tris(bipyridine)-

^aSchool of Chemistry, University of New South Wales, Sydney, NSW 2052, Australia. E-mail: p.thordarson@unsw.edu.au; Fax: +61-2-9385-6141; Tel: +61-2-9385-4478

^bAnalytical Centre, University of New South Wales, Sydney, NSW 2052, Australia †Electronic supplementary information (ESI) available: Terpyridine ligand synthesis, mono-complex synthesis, in-gel tryptic digest, photoreduction and quantum efficiency calculations, Ru(II)-cyt *c* bioconjugate structural model, UV-Vis/MALDI-TOF spectra of bioconjugates, ¹H/¹³C NMR spectra for novel compounds and selective crystallographic distances and angles. CCDC 931062 and 931063. For ESI and crystallographic data in CIF or other electronic format see DOI: 10.1039/c3ob40620b

ruthenium(II) complexes *via* functionalisation of histidine,¹³ lysine¹⁴ or cysteine residues.¹⁵ In contrast, electron transfer based on bis(terpyridine)ruthenium(II) complexes as electron donors have been limited. Hamachi *et al.*¹⁶ had reported room temperature electron transfer in apomyoglobin reconstituted with ruthenium bis(terpyridine) complex appended heme as the enzyme cofactor. Additionally, our group have previously reported light-activated bioconjugates involving iso-1 cytochrome *c* capable of electron transfer based on short and long chain spacer bis(terpyridine)ruthenium(II) complexes.

Herein, we describe a novel approach for improving the synthesis of light-activated ruthenium(II) and iridium(III) based cytochrome *c* bioconjugates including relevant single crystal structures of ruthenium(II) complexes Ru(II) **3** and Ru(II) **4**. We also demonstrate the membrane encapsulation of Ru(II)–cyt *c* bioconjugates in polystyrene-*b*-poly(acrylic acid) vesicles and how this enhances the photoreduction performance of the bioconjugate.

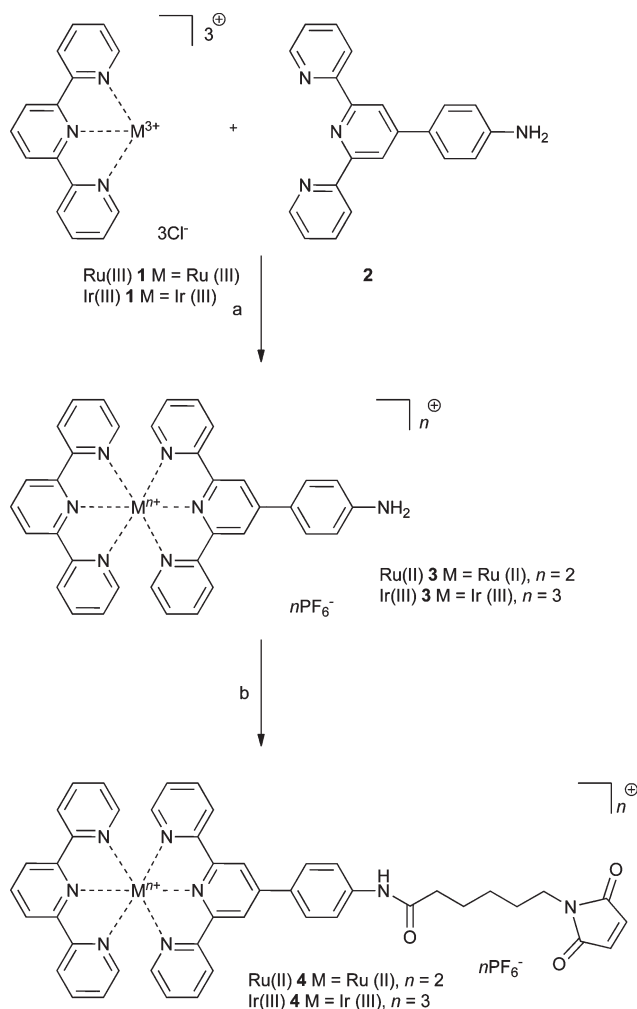
Results and discussion

Synthesis of complexes

All asymmetric Ru(II)/Ir(III) complexes were synthesised using a directed strategy in a two-step procedure to prevent “scrambling” of the terpyridine ligands. Complexes Ru(II) **1** and Ir(III) **1** were synthesised by heating the ruthenium(II) or iridium(III) chloride salt with 2,2':6',2''-terpyridine in absolute ethanol or neat ethylene glycol, respectively, following literature methods to yield a mono-complex.^{17,18} Subsequently, the second aniline terpyridine **2** ligand was heated with the mono-complexes Ru(II) **1** and Ir(III) **1** in ethylene glycol based on the method adapted from Collin *et al.* as shown in Scheme 1 to yield Ru(II) **3** and Ir(III) **3**.¹⁷

Generally, the Ru(II) mono-complex is reacted with the second ligand in ethanol (reductant) containing *N*-ethylmorpholine (catalyst)¹⁹ and refluxed to afford the bis(terpyridine) complex. Interestingly, it was found that in the presence of *N*-ethylmorpholine, complexation with aniline terpyridine **2** resulted in *N*-alkylation of the ligand. As a result of the poor yield due to the removal of catalyst in the complexation reaction of aniline **2**, the reaction was repeated using an alternative method based on Ir(III) bis(terpyridine) literature, using ethylene glycol as a solvent substitute²⁰ increasing the yield of Ru(II) **3** from 28% to 76%.

Maleimide functionalised complexes Ru(II) **4** and Ir(III) **4** were prepared for bioconjugation to cytochrome *c* *via* Michael addition. The maleimide functionality was introduced using conditions adapted from Hovinen²¹ due to the unreactive nature of the aniline derivatives Ru(II) **3** and Ir(III) **3** preventing the use of classical *N*-hydroxysuccinimide/*N,N'*-dicyclohexylcarbodiimide (NHS/DCC) coupling conditions. Maleimide functionalised Ru(II) **4** and Ir(III) **4** were prepared using the peptide coupling agent *O*-(7-azabenzotriazole-1-yl)-1,1,3,3-tetramethyluronium hexafluorophosphate (HATU) with *N,N*-diisopropylethylamine (DIPEA).



Scheme 1 Synthesis of maleimide functionalised Ru(II)/Ir(III)-bisterpyridines. (a) Ethylene glycol, 110 °C, Ru(II) **3**, 76%; Ir(III) **3**, 74%. (b) 6-Maleimidocaproic acid, *O*-(7-azabenzotriazole-1-yl)-1,1,3,3-tetramethyluronium hexafluorophosphate (HATU), *N,N*-diisopropylethylamine, DMF, r.t. Ru(II) **4**, 41%; Ir(III) **4**, 9.5%.

The complexes were purified using column chromatography on silica or alumina and characterised by high resolution ESI mass spectrometry. The most abundant molecular ion in mass spectrometry corresponded to complete loss of counter ions (PF_6^-), with the exception of Ru(II) **4**, resulting in a loss of two PF_6^- anions. Additionally, complexation was confirmed by UV-Vis spectroscopy showing the appearance of the characteristic metal-ligand charge transfer (MLCT) band. ¹H NMR spectroscopy confirmed complexation due to the characteristic upfield shift of the 6,6''-protons as a result of *anti* to *syn* conformation change of the terpyridine ligand. The Ru(II) **3** exhibited a typical shift, with a doublet observed at δ 8.73 ppm for aniline **2** shifted to δ 7.44 ppm for Ru(II) **3**.

X-ray structures of **1** and **2**

Red blades of Ru(II) **3** and Ru(II) **4** were crystallised by diffusion of diethyl ether vapour into *N,N'*-dimethylformamide solutions of the complexes. Ru(II) **3** was crystallised in the triclinic space group ($P\bar{1}$). As shown in Fig. 1, crystal Ru(II) **3** displays an

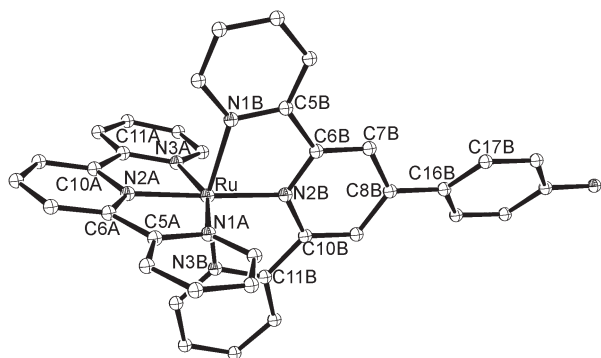


Fig. 1 ORTEP representation of the X-ray crystal structure of asymmetric Ru(II) **3** [Ru(C₁₅H₁₁N₃)(C₂₁H₁₆N₄)](PF₆)₂·2C₃H₇NO. Hydrogen atoms, PF₆⁻ anions and solvent molecules omitted for clarity and thermal ellipsoids are plotted as 20% probability.

orthorhombic distortion from octahedral symmetry (N2A–Ru–N3A 78.8(5)°) which is as expected and observed in [Ru(tpy)₂](PF₆)₂.²²

As shown in Table S1,[†] the Ru(II) **3** shows a significant twist with a torsional angle of 29.1(2)° (C7B–C8B–C16B–C17B) about the interannular bond, greater than the corresponding twist found in the free 4'-phenyl terpyridine ligand.²³ Ru–N bond lengths between ligands A and B are equivalent, 2.033(7) Å and is within reported ranges for [Ru(tpy)₂](PF₆)₂.²² The C–C and C–N bond lengths within the aromatic rings are normal and average 1.380(1) and 1.355(6) Å, respectively. The interannular C–C bond distances of ligands A and B average 1.464(5) and 1.474(7) Å and are consistent with reported asymmetric complex [Ru(tpy)(4'-5-carboxypentyl-tpy)](PF₆)₂ of 1.471(1) Å.¹⁷

Maleimide functionalised complex Ru(II) **4** was crystallised in the monoclinic space group (P2₁/c) with structural characteristics similar to that of Ru(II) **3**. The main notable difference is the reduction in the torsion angle between 4'-aryl maleimide group and the central pyridyl ring of ligand B with an angle of 23.9(8)° as shown in Table S1[†] and Fig. 2.

Synthesis of Ru(II)/Ir(III) bioconjugates

Light-harvesting bioconjugates Ru(II)/Ir(III)–cyt *c* were prepared for photoinduced electron transfer studies. Bioconjugation reactions involving the iso-1 form of cyt *c*, as shown in

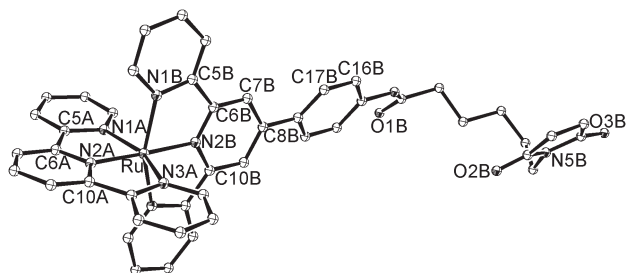
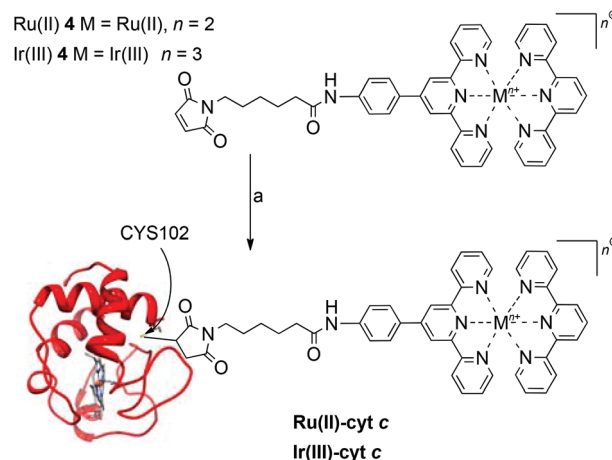


Fig. 2 X-ray crystal structure of the asymmetric Ru(II) **4** [(Ru(C₁₅H₁₁N₃)(C₃₁H₂₇N₅O₃))(PF₆)₂·2C₃H₇NO·H₂O. Hydrogen atoms, PF₆⁻ anions and solvent molecules omitted for clarity and thermal ellipsoids are plotted as 20% probability.



Scheme 2 Synthesis of Ru(II)/Ir(III)–cyt *c* bioconjugates. (a) Reduced iso-1 cytochrome *c* (10 μM), phosphate buffer (20 mM), ethylenediaminetetraacetic acid (20 mM), tris(2-carboxyethyl)-phosphine (TCEP, 5 μM), pH 7.0, acetonitrile (5% v/v), r.t. Ru(II)–cyt *c*, 27%; Ir(III)–cyt *c*, 33%.

Scheme 2 are desirable due to the presence of a single available cysteine residue at CYS102 for modification with maleimides allowing site-specific modification. The synthesis of bioconjugates followed previously optimised conditions in our group.⁷ The bioconjugate Ru(II)–cyt *c* was site-specifically reacted by using the maleimide functionalised Ru(II) **4**.

Iso-1 cytochrome *c* was added to a solution containing five-fold excess of Ru(II) **4** in a phosphate buffer at pH 7.0 containing ethylenediaminetetraacetic acid (EDTA) and acetonitrile. The final reaction conditions were iso-1 cytochrome *c* (10 μM), Ru(II) **4** (50 μM), phosphate buffer (20 mM), EDTA (20 mM) and acetonitrile (5% v/v) at pH 7.0 as shown in Scheme 2. The mixture was stirred overnight at room temperature in a plastic reaction vessel in the dark to prevent degradation of maleimide and photoreduction of cytochrome *c*. It should be noted that the addition of EDTA improves bioconjugation yields by removal of trace copper ions *via* chelation, as oxidation of cysteine can occur.²⁴

It was observed that with the hexafluorophosphate salt of Ru(II) **4**, significant precipitation of the complex was observed after stirring for 20 h resulting in extremely low yields <1%. However, it was noticed that after exchange with a chloride salt, improved water solubility of the complex Ru(II) **4** was observed with slight formation of precipitates. Subsequently, purification of conjugate Ru(II)–cyt *c* was achieved using similar conditions as previously developed in our group for Ru(II)-bis(terpyridine) based bioconjugates.⁶ Separation of covalently attached Ru(II)–cyt *c* from unreacted proteins and ligands can be achieved using Ni²⁺ immobilised IMAC chromatography, although the mechanism remains unknown.

In addition to increasing yields by increasing complex solubility with chloride counter-ion exchange, it was discovered that the addition of half an equivalent (to cyt *c*) of tris(2-carboxyethyl)-phosphine (TCEP) improved the bioconjugate yield (Ru(II)–cyt *c*) to a maximum of 27%, an approximate 20-fold increase. TCEP is a water soluble reducing agent and when

used in low concentration does not react with the maleimide functional group, unlike commonly used reducing agents such as dithiothreitol (DTT) and 2-mercaptoethanol. However, when used at an equivalent concentration to Ru(II) **4**, the reaction is inhibited due to the competing reaction of Ru(II) **4** with TCEP. This is in agreement with literature, as Schafer *et al.*²⁵ found that at pH 7, 50% of *N*-ethylmaleimide reacted with an equimolar amount of TCEP in 5 minutes. Hence, the cysteine residue (CYS102) of cyt *c* can oxidise to form sulfoxide species resulting in low yields. The presence of TCEP in the reaction mixture ensured that the CYS102 residue remained reduced and available for reactions with the maleimide functionalised complex Ru(II) **4** and Ir(III) **4**.

The bioconjugates were characterised using UV-Vis spectroscopy, MALDI-TOF mass spectrometry and gel electrophoresis (SDS-PAGE). Gel electrophoresis of Ru(II)-cyt *c*, as shown in Fig. 3 shows that the bioconjugate (lane 2) migrates as a slightly larger species than unmodified iso-1 cyt *c* (lane 1), which is as expected.

The Ir(III) **4** with the hexafluorophosphate anion was exchanged with chloride, which improved water solubility to such an extent that no acetonitrile was required to solubilise it in bioconjugation reactions. Bioconjugation was carried out under similar conditions to Ru(II)-cyt *c*, with 0.5 equivalent of TCEP (to cyt *c*). Similarly, purification of the reaction mixture followed the purification protocol of Ru(II)-cyt *c*. Characterisation of the Ir(III)-cyt *c* bioconjugate by UV-Vis, MALDI-TOF and gel electrophoresis showed incomplete removal of unreacted cyt *c* and Ir(III) **4**. Based on UV-Vis spectra, it is estimated that the purified fractions contained 20% of unreacted Ir(III) **4** (Fig. S5, ESI[†]). This is attributed to the strong non-

covalent interactions between cyt *c* and Ir(III)-bis(terpyridine) complexes which is discussed further in the next section.

As shown in Fig. 3, gel electrophoresis of Ir(III)-cyt *c* shows that the bioconjugate (lane 3) migrates as a slightly larger species than unmodified iso-1 cyt *c* (lane 1), which is as expected. Also, the presence of unreacted cyt *c* in Ir(III)-cyt *c* was also confirmed by gel electrophoresis, as a faint band can be discerned below the main band in lane 3. A faint band between 3 and 6 kDa was observed in lane 3. The identity of this band is not known. An in-gel tryptic digest of each band in this gel was inconclusive, only confirming that cyt *c* was present in all bioconjugate bands. The smaller molecular weight band may be a result of fragmentation of cyt *c* during bioconjugation and isolation.

Non-covalent binding between Ir(III) bis(terpyridine) and cyt *c*

Ir(III)-bis(terpyridine) complexes are capable of room temperature luminescence under aerated conditions. As such, Stern-Volmer analysis can be used to identify interactions between a fluorescent or phosphorescent probe and a quencher.^{26,27} To investigate possible non-covalent interactions between Ir(III) bisterpyridine complexes and iso-1 cyt *c*, the effect of cyt *c* concentration on the emission of a reference Ir(III) complex, Ir(III) **6** was examined as shown in Fig. 4.

Equimolar solutions of Ir(III) **6** with varying concentrations of cyt *c* were prepared and the emission intensity was recorded at 350 nm. The Stern-Volmer plot of emission intensity of Ir(III) **6** (4.3 μM) at 25 °C and 35 °C as a function of cyt *c* concentration is shown in Fig. 5.

Based on a simple 1 : 1 stoichiometric model and complete quenching upon complexation, the data corresponds to binding isotherms and can be analysed by non-linear regression to give an association constant (K_a) for the Ir(III) **6** : cyt *c* interaction.²⁸ This analysis gave association constants of $(3.5 \pm 0.6) \times 10^4 \text{ M}^{-1}$ at 25 °C and $(3.3 \pm 0.9) \times 10^4 \text{ M}^{-1}$ at 35 °C showing temperature independence on the binding of Ir(III) **6** to cyt *c*. The Stern-Volmer plot as shown in Fig. 5 is non-linear and displays an upward curvature concave towards the axis of ordinates and second order with respect to cyt *c* concentration. This is typical of a combination of static and dynamic binding.²⁷

Moreover, to further investigate the photoreduction rate previously observed for non-covalent mixtures of Ir(III) **6** and iso-1 cyt *c* in the presence of sacrificial donor

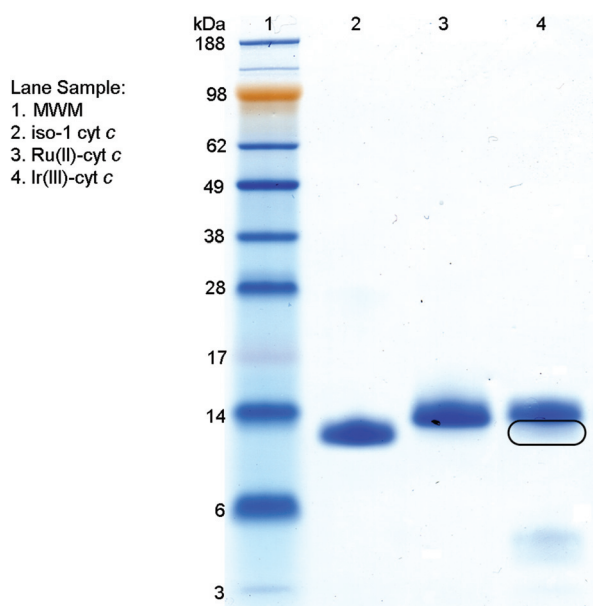


Fig. 3 Gel electrophoresis (reduced) of SeeBlue[®] Plus2 molecular weight marker (lane 1), iso-1 cytochrome *c* (lane 2, expected 12 706), Ru(II)-cyt *c* (lane 3, expected 13 559) and Ir(III)-cyt *c* (lane 4, expected 13 649). Samples are reduced with dithiothreitol (DTT). Samples stained with SimplyBlue[™] safestain.

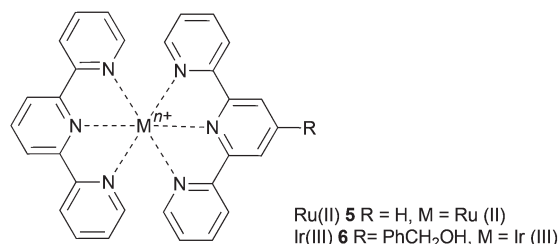


Fig. 4 Ru(II) and Ir(III) reference compounds used in this work.

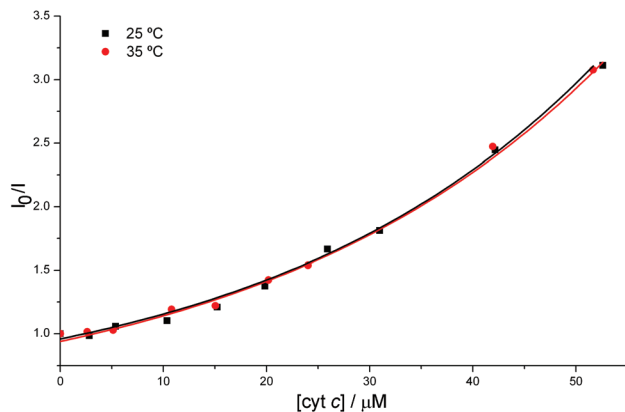


Fig. 5 Stern-Volmer plot of Ir(III) 6 (4.3 μM) emission intensity (at 25 °C and 35 °C) in the presence of cyt *c*.

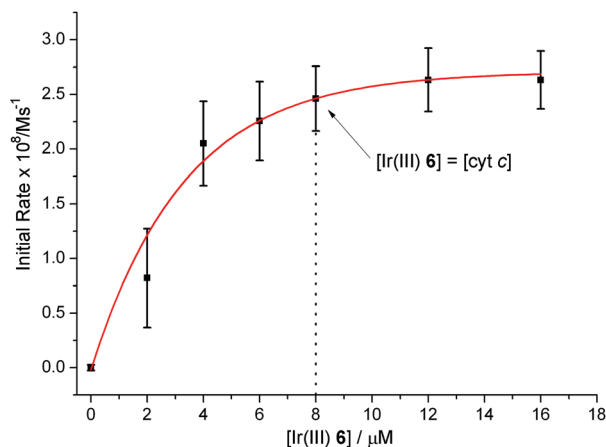


Fig. 6 The effect of Ir(III) 6 on the initial rate of cyt *c* heme reduction in non-covalent mixtures of Ir(III) 6, iso-1 cyt *c* (8 μM), EDTA (20 mM), phosphate buffer (20 mM), pH 7.0, 25 °C.

ethylenediaminetetraacetic acid (EDTA), the effect of Ir(III) concentration on the rate of cyt *c* heme reduction was studied as shown in Fig. 6.

As shown in Fig. 6, the initial rate of cytochrome *c* reduction is only dependent on the concentration of the Ir(III) bis(terpyridine) complex at low Ir(III) concentration (below 4 μM). No further increase in the initial rate of reduction is observed at concentrations greater than a $\sim 1:1$ ratio of Ir(III) to iso-1 cyt *c*, consistent with the applied $1:1$ binding constant model. The rapid reduction of cyt *c* under these conditions is believed to be due to both the non-covalent binding mechanism between the Ir(III) complex and iso-1 cyt *c*, as well as a secondary reduction mechanism by EDTA radicals.

Photoreduction studies of Ru(II)/Ir(III) bioconjugates

Our group has previously demonstrated room temperature photoinduced electron transfer in Ru(II)-bis(terpyridine)

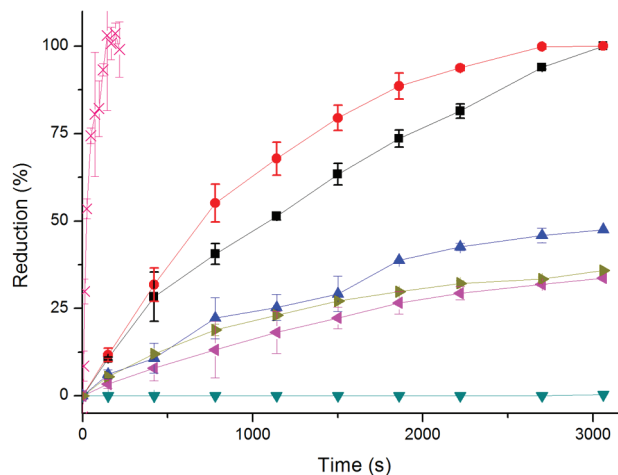


Fig. 7 Room temperature photoreduction of Ru(II)/Ir(III)-bis(terpyridine) based cyt *c* samples. All sample measurements were made at a concentration of $2.3 \pm 0.1 \mu\text{M}$ in 5 mM sodium dihydrogen phosphate, 5 mM ethylenediaminetetraacetic acid (EDTA), pH 7.0. Ru(II)-cyt *c* (■), Ru(II)-cyt *c*:polymersome (●), Ru(II)-cyt *c* non-degassed (▲), Ru(II)-cyt *c* no EDTA (▼), non-covalent (1:1) Ru(II) 5: cyt *c* mixture (◀), non-covalent (1:1) Ru(II) 5: cyt *c*:polymersome mixture (▶) and Ir(III)-cyt *c* (×). Error bars indicate standard deviation. Ru(II)/Ir(III)-bis(terpyridine) complexes irradiated with 465 nm or 372 nm light, respectively.

cytochrome *c* bioconjugates using a short and long chain spacer.⁶ It was found that long chain spacers resulted in optimum electron transfer as the use of short chain spacers caused inactivation of the protein.

Based on the findings of Peterson *et al.*,⁶ photoreduction studies of the novel long chain spacer bioconjugate Ru(II)-cyt *c* and non-covalent mixtures with reference Ru(II) 5 and iso-1 cyt *c* as shown in Fig. 4 and Scheme 2 were used to determine the effect of membrane encapsulation on photoreduction rates. Additionally, photoreduction studies were performed on bulk solution Ir(III)-cyt *c* to determine the effect of substituting a long-lived luminescence lifetime complex (Fig. 7).^{12,29}

In order to demonstrate light-activated electron transfer in bioconjugate Ru(II)-cyt *c*, samples were prepared in a specialised small volume cuvette, degassed and irradiated (2.5 cm) with a constant area at a bioconjugate concentration of $2.3 \pm 0.1 \mu\text{M}$ and an equivalent $1:1$ non-covalent mixture of Ru(II) 5 and iso-1 cyt *c* in a 5 mM phosphate buffer, 5 mM EDTA at pH 7.0 in either bulk solution or encapsulated in the PS₁₄₀-*b*-PAA₄₈ membrane. This experiment was also conducted under different conditions to determine the effect on heme reduction rate, including the presence of oxygen, the absence of sacrificial electron donor EDTA or the substitution of Ru(II) 4 with Ir(III) 4 of the corresponding bioconjugate.† It should be noted that concentrations used for photoreduction studies were low

†The concentrations were estimated by UV-Vis absorption spectroscopy with molar absorption coefficients: iso-1 cyt *c*/Ru(II)-cyt *c*/Ir(III)-cyt *c* ($\epsilon_{410} = 97.6 \text{ mM}^{-1} \text{ cm}^{-1}$)³⁹ and Ru(II) 5 ($\epsilon_{476} = 17.7 \text{ mM}^{-1} \text{ cm}^{-1}$).⁸

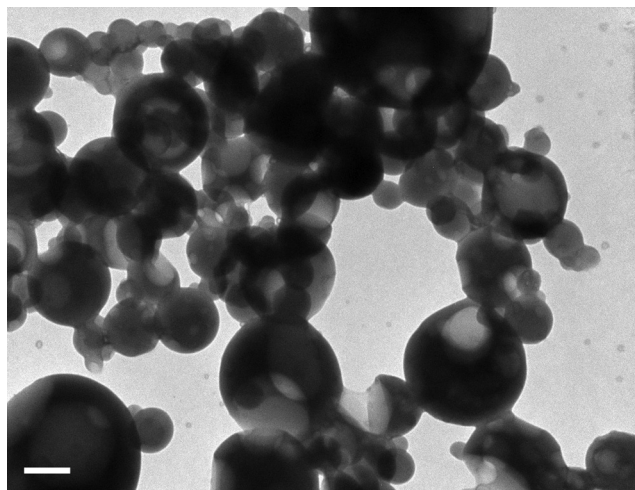


Fig. 8 TEM micrograph of polystyrene₁₄₀-*b*-poly(acrylic acid)₄₈ (PS₁₄₀-*b*-PAA₄₈) polymersome aggregates in the presence of 14 μM Ru(II)-cyt *c* in PBS (25 °C). Average polymersome diameter of 290 ± 132 nm. Scale bar: 200 nm.

to prevent intermolecular electron transfer in bioconjugate samples.

We have previously reported that positively charged proteins and peptides, including cyt *c*, are capable of inducing polymersome formation using the diblock copolymer PS₁₄₀-*b*-PAA₄₈ with concomitant encapsulation in the membrane.³⁰ To determine the effect of electron transfer after encapsulation within PS₁₄₀-*b*-PAA₄₈ polymersome membranes, the polymer aggregates were characterised by transmission electron microscopy (TEM) prior to room temperature photoreduction measurements to ensure that bioconjugate Ru(II)-cyt *c* induced polymersome formation. As shown in Fig. 8, polymersome aggregates were observed with an average diameter of 290 ± 132 nm.

As shown in Fig. 7, encapsulation of Ru(II)-cyt *c* resulted in an increase in initial rate of reduction of heme and fully reduced within 50 minutes. Encapsulation was estimated to be double the Φ of bulk solution Ru(II)-cyt *c* photoreduction with a Φ of $1.1 \pm 0.3 \times 10^{-3}\%$ over an estimated maximum distance between ruthenium and heme centre of ≤ 32 Å (Fig. S3, ESI†). The increase in Φ could be explained using semi-classical theory (Marcus-Hush theory of electron transfer) which describes electron tunnelling in proteins.^{31–33} It has been reported that embedding reactants in a membrane (low dielectric medium) dramatically reduces reorganisational energies, hence, the encapsulation of Ru(II)-cyt *c* in the polymersome membrane leads to an increase in electron transfer rate (k_{ET}).³² Another possibility leading to increased Φ may be due to the flexible linker used in Ru(II) **4** for attachment to cyt *c* allowing the complex to lie flat on the protein surface when embedded in the polyelectrolyte membrane. This decrease in distance between the donor and acceptor resulted in increased k_{ET} .³⁴

As shown in Table 1, it was observed that Ir(III)-cyt *c* had a Φ of $3.8 \pm 1.9 \times 10^{-1}\%$ in the bulk solution state,

Table 1 Estimated rates of heme reduction, reduction efficiency and quantum efficiency (Φ) for the photoinduced reduction of Ru(II)-cyt *c*/Ir(III)-cyt *c* systems

Sample ^a	λ (nm)	Heme reduction (electrons per second) ^b	Efficiency ^{i,c} (%) (electrons/photons)	Φ^d (%) (electrons/absorbed photons)
Ru(II)-cyt <i>c</i> ^e	465	$7.9 \pm 1.8 \times 10^9$	$5.6 \pm 0.9 \times 10^{-5}$	$5.9 \pm 1.5 \times 10^{-4}$
Ru(II)-cyt <i>c</i> ^f	465	$1.5 \pm 0.3 \times 10^{10}$	$1.1 \pm 0.3 \times 10^{-4}$	$1.1 \pm 0.3 \times 10^{-3}$
Ir(III)6 : cyt <i>c</i> ^{e,g}	465	$4.6 \pm 0.6 \times 10^9$	$3.3 \pm 0.6 \times 10^{-5}$	$3.4 \pm 0.6 \times 10^{-4}$
Ir(III)6 : cyt <i>c</i> ^{f,g}	465	$5.1 \pm 1.3 \times 10^9$	$3.6 \pm 1.0 \times 10^{-5}$	$3.8 \pm 1.1 \times 10^{-4}$
Ir(III)-cyt <i>c</i> ^{e,h}	372	$6.6 \pm 0.4 \times 10^{11}$	$3.0 \pm 1.5 \times 10^{-2}$	$3.8 \pm 1.9 \times 10^{-1}$

^a Sample concentration of 2.3 ± 0.1 μM in 5 mM sodium dihydrogen phosphate, 5 mM EDTA, pH 7.0 at 25 °C with 80 μL volume. Irradiated with 20 ± 2.3 mW cm⁻² of 465 nm light or 0.04 ± 0.02 mW cm⁻² of 372 nm light. ^b Initial rate of heme reduction was estimated using amount of protein reduced in the first 1860 s interval. ^c Efficiency (%) was determined by dividing initial rate of heme reduction by incident photons. ^d Quantum efficiency was determined by correcting for the optical density of the solutions (Fig. S2, ESI). ^e Bulk solution measurement. ^f Encapsulated measurement in PS₁₄₀-*b*-PAA₄₈ membrane. ^g Non-covalent mixture. ^h 120 μL volume. Errors are standard deviation. ⁱ Incident photons are $1.40 \pm 0.2 \times 10^{16}$ photons s⁻¹ for 465 nm light or $2.2 \pm 1.1 \times 10^{13}$ photons s⁻¹ for 372 nm light. Incident photons calculated from power output over an irradiation area of 1.0×0.3 cm for the light source.

corresponding to a ~650-fold increase in quantum efficiency relative to bulk Ru(II)-cyt *c*. This significant improvement may be due to the longer luminescence lifetime of Ir(III)-bis(terpyridine) complexes at room temperature.^{12,29}

To determine the effect of covalent linkage of Ru(II)-bis(terpyridine) donor to cyt *c*, non-covalent studies using a 1 : 1 mixture of reference complex Ru(II) **5** and cyt *c* in bulk solution or encapsulated in membrane were performed in the presence of EDTA and degassed. Ru(II) **5** was chosen as a control complex compared to Ru(II) **4** as the lack of maleimide functionality prevents reaction with protein. It was observed in Fig. 7 that a dramatic decrease in photoreduction yield resulted in non-covalent mixtures. This indicates that covalent attachment to protein is essential to ensure proximity between donor and acceptor to increase photoreduction efficiency. However, the behaviour of increasing Φ was observed after encapsulation, consistent with covalent bioconjugate Ru(II)-cyt *c* studies. The reduction efficiencies and quantum efficiencies of bioconjugate Ru(II)-cyt *c* and non-covalent mixtures in bulk solution and membrane encapsulation is summarised in Table 1.

Photoexcitation of Ru(II)-bis(terpyridine) to the triplet metal-to-ligand charge-transfer (³MLCT) state is short lived and non-luminescent at room temperature with an excited-state lifetime estimated to be 250 ps.³⁵ To investigate if the presence of oxygen significantly quenches the excited chromophore Ru(II)*, photoreduction studies were performed without degassing. A quenching of photoreduction by ~50% was observed in non-degassed experiments as shown in Fig. 7. Additionally, the presence of sacrificial electron donor, EDTA, is essential as bioconjugate Ru(II)-cyt *c* in phosphate buffer shows negligible photoreduction as shown in Fig. 7.

Conclusions

Ruthenium(II) and iridium(III) bis(terpyridine) complexes were prepared with maleimide functionalities in order to site-specifically modify yeast iso-1 cytochrome *c* possessing a single cysteine residue available for modification (CYS102). Single X-ray crystal structures were solved for aniline and maleimide complexes Ru(II) **3** and Ru(II) **4**, respectively, providing detailed structural detail of the complexes. Light-activated bioconjugates prepared from Ru(II) **4** and Ir(III) **4** were prepared allowing for room temperature photoinduced electron transfer studies. It was observed that strong binding between Ir(III) bis(terpyridine) complexes and cyt *c* occurred, confirmed *via* titration and Stern–Volmer studies with Ir(III) **6**. As a result of the high binding affinities between Ir(III) bis(terpyridine) complexes and cyt *c*, difficulties in isolation of Ir(III)–cyt *c* were encountered resulting in ~20% of Ir(III) **4** present in the Ir(III)–cyt *c* bioconjugate mixture.

Photoinduced electron transfer studies of Ru(II)–cyt *c* in bulk solution and polymer membrane encapsulated specimens were performed using EDTA as a sacrificial electron donor. It was found that membrane encapsulation of Ru(II)–cyt *c* in PS₁₄₀-*b*-PAA₄₈ resulted in a two-fold increase of the quantum efficiencies. Moreover, Ir(III)–cyt *c* bioconjugates showed a ~640-fold increase in quantum efficiencies relative to Ru(II)–cyt *c*. The bioconjugates allow photo-switchability between on/off states controlling the reduction of cyt *c*. The biohybrids potentially will allow scientists to drive biological processes *via* room temperature photoinduced electron transfer. Potential applications include the encapsulation in artificial capsules and vesicles as a component of an artificial electron transport chain to drive chemical reactions or energy gradients as nano-reactors or artificial cells.^{36–38}

Experimental

Chemicals, solvents and materials

Chemicals were purchased from Sigma Aldrich with the exceptions of ammonium acetate, sodium dihydrogen phosphate, sodium hydroxide, sodium bicarbonate, anhydrous sodium sulphate, citric acid, iodine, pyridine and hydrazine monohydrate were purchased from Ajax Finechem Pty. Ltd, 4-nitrobenzaldehyde (Hopkins and Williams Ltd), ammonium hexafluorophosphate (Acros Organics) and ruthenium(III) trichloride hydrate (Precious Metals Online). Silica was purchased from Davisil (40–63 μM). Thin layer chromatography plates (Kieselgel 60 F-254 pre-coated sheets 0.25 mm) were purchased from Merck. Neutral alumina oxide was purchased from Merck (Alumina Oxide 90 active neutral, 20–230 mesh). Dichloromethane (CH₂Cl₂) and methanol (CH₃OH) were distilled before use. Dry solvents such as acetonitrile (CH₃CN), dichloromethane, diethyl ether (Et₂O) and tetrahydrofuran (THF) were obtained from a Pure Solv dry solvent system (Innovative Technology, Inc., model #PS-MD-7). Dry methanol was distilled and stored over calcium chloride. Dry *N,N*-

dimethylformamide (DMF) was purchased from Sigma Aldrich and used directly from the bottle. Deuterated solvents for NMR were obtained from Cambridge Isotope Laboratories. For aggregation studies and preparation of all salt buffers, ultra pure water ($R > 18 \times 10^6 \Omega$) was used. Water and organic solvent was filtered through a 0.45 μm cellulose membrane filter (Minisart RC 25, Sartorius Stedim Biotech) prior to polymer aggregation studies. Diblock copolymer, polystyrene₁₄₀-*b*-poly(acrylic acid)₄₈ (PDI = 1.10), was purchased from Encapson (The Netherlands, catalogue number 1036). All other chemicals were used as received.

Yeast cytochrome *c* from *Saccharomyces cerevisiae* (catalogue number C2436) was purchased from Sigma Aldrich. Yeast iso-1 cytochrome *c* was purified following previously published procedures prior to bioconjugation reactions.^{7,39} Buffer pH values were monitored using a Scholar 425 pH meter (Corning) and filtered using a 0.45 μm (Millipore, 47 mm regenerated cellulose) prior to use.

A Varian Cary 50 Bio UV-Vis or Cary 5 UV-Vis-NIR spectrometer was used for UV-Vis spectra measurements. Fluorescence spectra were recorded using a Varian Cary Eclipse spectrometer with excitation and emission slits at 5 nm, excitation filter “auto”, emission filter “open” and PMT voltage set to “medium”, unless otherwise stated. NMR spectra (¹H and ¹³C) were recorded in the designated solvents using a Bruker Avance DPX (300 MHz) spectrophotometer. Chemical shifts are measured in parts per million (ppm), internally referenced relative to tetramethylsilane (SiMe₄, ¹H and ¹³C = 0 ppm) or residual solvent peaks (CD₃CN: ¹H = 1.94 and ¹³C = 1.32; DMSO-*d*₆: ¹H = 2.50, ¹³C = 39.52; CDCl₃: ¹H = 7.26 ppm, ¹³C = 77.16 ppm). IR spectra were recorded on a Shimadzu FTIR-8400S, ThermoNicolet Avatar model 370 FT-IR or a Perkin Elmer Spotlight 400 FT-IR spectrometer equipped with a microscope and attenuated total reflectance (ATR) accessories with diamond crystal inset. Low resolution electrospray ionisation (ESI) mass spectra were recorded on a Waters Micro-mass ZQ electrospray instrument. High resolution ESI mass spectrometry was performed on a Thermo Linear Quadrupole Ion Trap Fourier Transform Ion Cyclotron Resonance (LQT FT Ultra) mass spectrometer in electrospray mode with a 7 T superconducting magnet. MALDI-TOF mass spectra were recorded on an Applied Biosystems Voyager DE STR MALDI reflectron TOFMS (protein and bioconjugate measurements were made in linear mode). Melting points were recorded on a Mel-temp II hot stage apparatus. TEM micrographs were recorded on a JEOL 1400 (80 kV) instrument.

Protein and bioconjugate purification was performed using a GE Healthcare ÄKTApurifier. Cation exchange chromatography (CEX) was performed using a strong cation exchange column (TSKgel SP-5PW, Supelco). Immobilised metal affinity chromatography (IMAC) was performed using either a Ni²⁺ charged HisTrap HP (GE Healthcare, 1 mL) or an Acrosep Hypercel (Pall, 1 mL) column. Protein solutions were concentrated using 3000 molecular weight cut-off (MWCO) centrifuge concentrators (Amicon Ultra-15, Amicon Ultra-4 or Amicon Ultra-0.5, Millipore). Samples were dialysed into MilliQ water

using Slide-A-Lyzer Mini Dialysis Units (3500 MWCO, Pierce) or Tube-O-Dialyzer Dialysis Units (4000/50 000 MWCO, G Biosciences).

Ru(II)/Ir(III)-cyt *c* bioconjugate photo-reactions were performed using a 16 LED Blue (465 nm) Flashlight (LDP LLC) or a 16 LED White (372 nm) Flashlight (LDP LLC), respectively. Power measurements of LED Flashlights were made using a Newport Power Meter (Model 1918-C).

Gel electrophoresis

Gel electrophoresis was performed using Invitrogen Novex® NuPage® 12% Bis-Tris, 1 mm, 10-well gels, SeeBlue® Plus2 molecular weight marker, NuPage® LDS sample buffer (4×), NuPage® sample reducing agent (10×), NuPage® MES SDS running buffer, SimplyBlue™ safestain and the gels run using a Zoom Dual Power supply (model ZP10002, Invitrogen). Samples for gel electrophoresis were prepared by dilution in Novex® NuPage® LDS sample buffer (Invitrogen). Samples were reduced (to eliminate disulfide dimers) by adding NuPage® sample reducing agent (active ingredient dithiothreitol (DTT)). Samples were heated at 70 °C for 10 min to denature the protein. Novex® NuPage® gels (12% Bis-Tris, 10-wells) were then loaded with 1–3 µg of protein per well, run at a constant 200 V for 40 min and stained according to the procedure included with SimplyBlue™ safestain.

Transmission electron microscopy (TEM) studies

TEM samples were prepared by placing 20 µL of sample onto a formvar-coated copper grid and the excess water was blotted away after 2 min with a filter paper. For statistical analysis, a population of 100 polymersomes were measured from TEM micrographs for determination of the average and standard deviation of diameters.

X-ray crystallography

Crystal growth of Ru(II)-bis(terpyridine) complexes. In general, Ru(II)-bis(terpyridine) complex (*ca.* 5 mg) was dissolved in minimal solvent (DMF) resulting in a concentrated solution. Crystals were grown by slow diffusion of anhydrous diethyl ether into a solution of complex in *N,N*-dimethylformamide at room temperature or 4 °C for Ru(II) 3 and Ru(II) 4, respectively. A suitable single crystal was selected under a polarising microscope (Leica M165Z) for single crystal X-ray diffraction analysis.

X-ray structure determination of Ru(II) 3. The X-ray diffraction measurement for Ru(II) 3 was performed on a Bruker kappa APEX-II CCD diffractometer at 150 K by using graphite-monochromated Mo-K α radiation ($\lambda = 0.71075$ Å). The crystal was mounted on the goniometer using cryo loops for intensity measurements, coated with paraffin oil and immediately transferred to the cold stream using Oxford Cryostream 700 system attachment. Upon obtaining an initial refinement of unit cell parameters, the data collection strategy was calculated to achieve a redundancy of at least 4 throughout the resolution range (∞ –0.80 Å) at 10 s exposure time per frame utilising the kappa offsets on the four circle goniometer geometry. Data

integration, reduction with multi-scan absorption correction method was carried out using Bruker APEX2 Suite software.⁴⁰ The structure was solved by Direct Methods program SHELXS-97 and refined by full-matrix least-squares refinement program SHELXL.⁴¹ All non-hydrogen atoms were refined anisotropically and hydrogen atoms were included by using a riding model. Further information is available in the ESI CIF files.†

X-ray structure determination of Ru(II) 4. The X-ray diffraction measurement for Ru(II) 4 was carried out at MX1 beamline at the Australian Synchrotron Facility, Melbourne. The crystal was mounted on the goniometer using cryo loop for intensity measurements, coated with paraffin oil and immediately transferred to the cold stream using a Cryostream attachment. Data was collected using Si<111> monochromated synchrotron X-ray radiation ($\lambda = 0.71023$ Å) at 100(2) K and was corrected for Lorentz and polarization effects using the XDS software.⁴² The structure was solved by Direct methods and the full-matrix least-squares refinements was carried out using SHELXL.⁴¹ Further information is available in the ESI CIF files.†

[Ru(tpy)(4'-(4-aminophenyl)-2,2':6',2''-tpy)](PF₆)₂ (Ru(II) 3)

Method 1. A solution of 4'-(4-aminophenyl)-2,2':6',2''-terpyridine 2 (273.3 mg, 0.8425 mmol) and [Ru(tpy)]Cl₃ 1 (373.6 mg, 0.8447 mmol) in ethylene glycol (50 mL) was heated to 110 °C for 20 h under nitrogen. Reaction mixture was diluted to 150 mL with water and filtered over celite. Filtrate was precipitated using ammonium hexafluorophosphate, washed with water (3 × 50 mL) and collected with acetonitrile. Purified over silica using a gradient from 90 : 9 : 1 CH₃CN : H₂O : KNO₃ (saturated) to 20 : 3 : 1 CH₃CN : H₂O : KNO₃ (saturated). Fractions precipitated with ammonium hexafluorophosphate and washed with water. Product further purified over alumina (neutral) using a gradient from acetonitrile to 90 : 9 : 1 CH₃CN : H₂O : KNO₃ (saturated). Fractions pooled, precipitated with ammonium hexafluorophosphate, washed with water (3 × 20 mL) and collected with acetonitrile yielding Ru(II) 3 as a red solid (609.6 mg, 76%). Mp >274 °C (decomposed); ¹H NMR (300 MHz, CD₃CN) δ 8.90 (s, 2H), 8.72 (d, *J* = 7.9 Hz, 2H), 8.60 (d, *J* = 7.9 Hz, 2H), 8.48 (d, *J* = 7.9 Hz, 2H), 8.38 (t, *J* = 8.3 Hz, 1H), 8.00 (dt, *J* = 8.6, 2.4 Hz, 2H), 7.91 (tt, *J* = 7.9, 1.3 Hz, 4H), 7.44 (dd, *J* = 4.9, 0.8 Hz, 2H), 7.30 (dd, *J* = 4.5, 0.8 Hz, 2H), 7.21–7.09 (m, 4H), 6.95 (dt, *J* = 8.7, 2.4 Hz, 2H); ¹³C NMR (75 MHz, CD₃CN) δ 159.1, 156.5, 156.0, 153.5, 153.3, 144.9, 138.9, 136.4, 129.8, 128.4, 128.2, 125.3, 124.6, 120.9, 115.8; IR (ATR) ν_{max} /cm⁻¹ 3646 (w), 3593 (w), 3506 (w), 3414 (w), 3121 (w), 1990 (w), 1633 (m), 1597 (m), 1529 (w), 1430 (m); UV-Vis (CH₃CN) λ_{max} /nm (ϵ /M⁻¹ cm⁻¹) 490 (1.71 × 10⁴), 364 (9.80 × 10³), 308 (5.00 × 10⁴), 283 (2.55 × 10⁴), 272 (2.86 × 10⁴), 231 (2.67 × 10⁴); HRMS (ESI) *m/z*: ([M – PF₆])⁺ calcd for C₃₆H₂₇N₇P₁F₆Ru⁺, 804.1023; found, 804.1006. MS (ESI) *m/z*: ([M – 2PF₆])²⁺ calcd for C₃₆H₂₇N₇Ru²⁺, 329.57; found, 329.49.

Method 2. A solution of 4'-(4-aminophenyl)-2,2':6',2''-terpyridine 2 (179.0 mg, 0.5518 mmol) and [Ru(tpy)]Cl₃ 1 (248.8 mg, 0.5645 mmol) in ethanol (100 mL) was refluxed for 20 h under nitrogen. Reaction mixture was filtered over celite, concentrated

in vacuo and diluted with water (100 mL). Filtrate was precipitated using ammonium hexafluorophosphate, washed with water (3 × 50 mL) and collected with acetonitrile. The product was recrystallised with acetonitrile/diethyl ether yielding Ru(II) 3 as a red solid (138.7 mg, 28%). Characterisation data was identical to the compound obtained from method 1 above.

[Ru(tpy)(maleimide-hexylcarboxamido-phenyl-tpy)](PF₆)₂ (Ru(II) 4)

A solution of 6-maleimidocaproic acid (53.2 mg, 0.252 mmol), *O*-(7-azabenzotriazole-1-yl)-1,1,3,3-tetramethyluronium hexafluorophosphate (HATU, 95.9 mg, 0.252 mmol) and *N,N*-diisopropylethylamine (66.8 mg, 0.517 mmol) in dry dimethylformamide (5 mL) was stirred at room temperature under nitrogen for 1 h. Subsequently, Ru(II) 3 (71.7 mg, 0.0756 mmol) in dry dimethylformamide (5 mL) was added to the mixture and stirred for a further 26 h in the dark at room temperature under nitrogen. Dichloromethane (50 mL) was added to the solution and the organic phase washed with aqueous citric acid (10% w/v, 2 × 20 mL), water (3 × 10 mL) and dried over anhydrous sodium sulphate. Dichloromethane was removed *in vacuo* and the concentrated red dimethylformamide phase containing product was precipitated from dry diethyl ether and the solid collected by filtration, washed with diethyl ether and collected with acetonitrile. Product was purified over silica using a gradient from acetonitrile to 70 : 29 : 1 CH₃CN : H₂O : KNO₃ (saturated). Fractions pooled, precipitated with ammonium hexafluorophosphate, washed with water (3 × 20 mL) and collected with acetonitrile yielding Ru(II) 4 as a red solid (27.9 mg, 41%). Mp >246 °C (decomposed); ¹H NMR (300 MHz, CD₃CN) δ 8.98 (s, 2H), 8.75 (d, *J* = 8.3 Hz, 3H), 8.63 (d, *J* = 7.9 Hz, 2H), 8.50 (d, *J* = 7.9 Hz, 2H), 8.40 (t, *J* = 8.3 Hz, 1H), 8.16 (dd, *J* = 8.7, 1.5 Hz, 2H), 8.00–7.85 (m, 6H), 7.43 (dd, *J* = 5.6, 0.8 Hz, 2H), 7.37 (dd, *J* = 6.4, 0.8 Hz, 2H), 7.20–7.10 (m, 3H), 6.75 (s, 2H), 3.49 (t, *J* = 7.0 Hz, 2H), 2.41 (t, *J* = 7.4 Hz, 2H), 1.80–1.56 (m, 5H), 1.45–1.33 (m, 2H); ¹³C NMR (75 MHz, CD₃CN) δ 173.60, 172.51, 159.49, 159.41, 159.26, 156.56, 153.61, 153.48, 149.09, 142.43, 139.19, 136.87, 135.37, 132.53, 129.51, 128.61, 128.56, 125.64, 125.56, 124.85, 122.17, 121.17, 38.44, 37.76, 29.17, 27.21, 25.94; IR (ATR) ν_{max}/cm⁻¹ 3647 (w), 3403 (w), 3112 (w), 2933 (w), 2857 (w), 1769 (w), 1699 (s), 1595 (m), 1523 (m), 1449 (m), 1407 (m); UV-Vis (CH₃CN) λ_{max}/nm (ε/M⁻¹ cm⁻¹) 485 (2.60 × 10⁴), 410 (4.88 × 10³), 308 (7.85 × 10⁴), 282 (4.32 × 10⁴), 272 (4.65 × 10⁴); HRMS (ESI) *m/z*: ([M - PF₆])⁺ calcd for C₄₆H₃₈N₈O₃P₁F₆Ru⁺, 997.1618; found, 997.1741 and ([M - 2PF₆])²⁺ calcd for C₄₆H₃₈N₈O₃Ru²⁺, 426.0988; found, 426.1050. MS (ESI) *m/z*: ([M - 2PF₆])²⁺, 426.11.

Prior to bioconjugation, Ru(II) 4 was exchanged with chloride salt to increase solubility and yield.

[Ir(tpy)(4'-(4-aminophenyl)-2,2':6'2''-tpy)](PF₆)₃ (Ir(III) 3)

[Ir(tpy)]Cl₃ 1 (170.0 mg, 0.320 mmol) and 4'-(4-aminophenyl)-2,2':6'2''-terpyridine 2 (101.3 mg, 0.312 mmol) were crushed together with a glass rod in a round-bottomed flask. Ethylene glycol was added (15 mL) and the reaction mixture was

degassed with three freeze-thaw cycles, heated to 160 °C under nitrogen in the dark, and stirred at this temperature for 15 minutes. The mixture was left to cool before the addition of aqueous ammonium hexafluorophosphate (90 mL). The resulting precipitate was centrifuged, washed with aqueous ammonium hexafluorophosphate (10 mL), absolute ethanol (3 × 10 mL), diethyl ether (3 × 10 mL), and recrystallised twice from acetonitrile and diethyl ether to yield Ir(III) 3 (272 mg, 74%) as an orange solid. Mp >300 °C; ¹H NMR (300 MHz, CD₃CN) δ 8.93 (s, 2H), 8.87–8.71 (m, 3H), 8.67 (ddd, *J* = 8.2, 1.4, 0.7 Hz, 2H), 8.57 (ddd, *J* = 8.1, 1.4, 0.7 Hz, 2H), 8.26–8.14 (m, 4H), 8.06 (d, *J* = 8.8 Hz, 2H), 7.69 (ddd, *J* = 5.7, 1.4, 0.6 Hz, 2H), 7.54 (ddd, *J* = 5.7, 1.5, 0.7 Hz, 2H), 7.52–7.40 (m, 4H), 6.97 (d, *J* = 8.8 Hz, 2H), 5.06 (s, 2H); ¹³C NMR (75 MHz, CD₃CN) δ 154.8, 154.3, 154.2, 143.8, 143.6, 131.0, 130.7, 130.4, 128.3, 128.0, 127.5, 122.5, 115.7; IR (ATR) ν_{max}/cm⁻¹ 3436 (br), 3063 (w), 2924 (w), 2857 (w), 1605 (s), 1474 (m), 1403 (m), 1241 (m), 1103 (m), 1051 (m), 824 (s, PF₆); HRMS (ESI) *m/z*: ([M - PF₆])⁺ calcd for C₃₆H₂₇N₇P₂F₁₂Ir⁺, 1040.1241; found, 1040.1236. MS (ESI) *m/z*: ([M - 2PF₆])²⁺ calcd for C₃₆H₂₇F₆N₇PIr²⁺, 447.58; found, 447.40.

[Ir(tpy)(maleimide-hexylcarboxamido-phenyl-tpy)](PF₆)₃ (Ir(III) 4)

A solution of 6-maleimidocaproic acid (78.5 mg, 0.372 mmol), HATU (142.2 mg, 0.372 mmol) and *N,N*-diisopropylethylamine (109.5 mg, 0.847 mmol) in dry dimethylformamide (7.5 mL) was stirred at room temperature under nitrogen for 1 h. Ir(III) 3 (129.6 mg, 0.112 mmol) in dry dimethylformamide (7.5 mL) was then added to the reaction mixture, which was stirred at room temperature under nitrogen in the dark for 25 h. Dichloromethane (75 mL) was added to the mixture, which was subsequently washed with aqueous citric acid (10% w/v, 2 × 30 mL) and water (3 × 20 mL). The aqueous phase was back-extracted with dichloromethane (2 × 30 mL), and the organic phases were pooled, dried over anhydrous sodium sulphate, and the dichloromethane removed *in vacuo*. The red dimethylformamide phase containing product was precipitated into diethyl ether, and the solid was centrifuged, washed with diethyl ether (2 × 5 mL), dissolved in acetonitrile, recrystallised into diethyl ether and the crude solid purified *via* column chromatography (silica, 20 : 3 : 1 CH₃CN : H₂O : KNO₃ (saturated)) to yield Ir(III) 3 (11.2 mg, 9.5%) as an orange-yellow solid. Mp >220 °C (decomposed); ¹H NMR (300 MHz, CD₃CN) δ 9.03 (s, 2H), 8.89–8.73 (m, 3H), 8.69 (ddd, *J* = 8.9, 1.7, 1.0 Hz, 2H), 8.58 (ddd, *J* = 8.1, 1.4, 0.7 Hz, 2H), 8.29–8.12 (m, 6H), 8.03–7.96 (ddd, 2H), 7.68 (ddd, *J* = 5.7, 1.5, 0.6 Hz, 2H), 7.57 (ddd, *J* = 5.7, 1.5, 0.6 Hz, 2H), 7.53–7.42 (m, 4H), 6.75 (s, 2H), 3.49 (t, *J* = 7.0 Hz, 2H), 2.42 (t, *J* = 7.4 Hz, 2H), 1.67 (ddt, *J* = 29.9, 14.8, 7.3 Hz, 4H), 1.46–1.27 (m, 2H); ¹³C NMR (75 MHz, CD₃CN) δ 173.08, 159.00, 158.85, 155.31, 154.35, 154.23, 144.60, 143.78, 143.71, 135.16, 130.71, 130.58, 130.42, 130.23, 128.31, 128.19, 127.52, 124.37, 120.78, 38.21, 37.60, 28.93, 26.94, 25.56; IR (ATR) ν_{max}/cm⁻¹ 3637 (w), 3390 (w), 3987 (w), 2925 (w), 2850 (w), 1751 (w), 1703 (s), 1591 (m), 1524 (m), 1479 (m), 1453 (m), 1412 (m), 1360 (m), 1315 (m), 1252 (m), 1188 (m); UV-Vis (H₂O) λ_{max}/nm (ε/M⁻¹ cm⁻¹) 377 (1.57 × 10⁴),

355 (1.77×10^4), 323 (2.58×10^4), 278 (3.93×10^4), 252 (4.03×10^4); HRMS (ESI) m/z : $[(M - 3Cl)]^{3+}$ calcd for $C_{46}H_{38}N_8O_3Ir^{3+}$, 314.4232; found, 314.4225; MS (ESI) m/z : $[(M - 3Cl)]^{3+}$, 314.15.

Prior to bioconjugation, Ir(III) **4** was exchanged with chloride salt to increase solubility and yield.

[Ru(tpy)₂](PF₆)₂ (Ru(II) **5**)¹⁷

A solution of 2,2':6',2''-terpyridine (113.8 mg, 0.488 mmol) and ruthenium(III) trichloride hydrate (49.6 mg, 0.239 mmol) in ethylene glycol (33 mL) was heated at 110 °C for 21 h. The solution was then diluted with water (150 mL), filtered through celite and the product was precipitated with ammonium hexafluorophosphate. The solid was collected by centrifugation, washed with water and recrystallised with acetonitrile/diethyl ether and collected by filtration and washed with acetonitrile yielding [Ru(tpy)₂](PF₆)₂Ru(II) **5** as a red solid (103.1 mg, 50%). ¹H NMR (300 MHz, CD₃CN) δ 8.73 (d, $J = 8.1$ Hz, 4H), 8.48 (dt, $J = 8.1, 1.0$ Hz, 4H), 8.40 (t, $J = 8.3$ Hz, 2H), 7.91 (td, $J = 7.8, 1.5$ Hz, 4H), 7.32 (dq, $J = 5.6, 0.8$ Hz, 4H), 7.19–7.11 (m, 4H). MS (ESI) m/z : $[(M - 2PF_6)]^{2+}$ calcd for $C_{30}H_{22}N_6Ru^{2+}$, 284.05; found, 283.80. These results are in agreement with those reported in the literature.¹⁷

[Ir(tpy)(4'-(4-hydroxymethylphenyl)-tpy)](PF₆)₃ (Ir(III) **6**)

[Ir(tpy)]Cl₃ **1** (100 mg, 0.183 mmol) salt and 4'-(4-hydroxymethylphenyl)-2,2':6',2''-terpyridine⁴³ (67 mg, 0.198 mmol) were crushed together with a glass rod. Ethylene glycol (15 mL) was added and the mixture degassed with three freeze–thaw cycles before being heated to 160 °C in the dark and under nitrogen for 20 min. The reaction mixture was allowed to cool to room temperature before an aqueous solution of excess ammonium hexafluorophosphate was added. The resulting precipitate was collected by filtration and washed with water, ethanol and diethyl ether, followed by recrystallisation from acetonitrile/diethyl ether. This was then purified by column chromatography (silica, 70 : 29 : 1, CH₃CN : H₂O : KNO₃ (saturated)), followed by precipitation using aqueous ammonium hexafluorophosphate, filtered, and recrystallised from acetonitrile/diethyl ether to yield Ir(III) **6** as a yellow solid (195 mg, 88%). Mp >300 °C; ¹H NMR (300 MHz, CD₃CN): δ 9.07 (s, 2H), 8.85 (d, 2H, $J = 8.8$ Hz), 8.80–8.70 (m, 3H), 8.59 (dd, 4H, $J = 7.5, 0.7$ Hz), 8.26–8.18 (m, 6H), 7.77 (d, 2H, $J = 7.7$ Hz), 7.69 (dd, 2H, $J = 5.7, 0.8$ Hz), 7.58 (dd, 2H, $J = 4.3, 0.5$ Hz), 7.52–7.45 (m, 4H), 4.82 (s, 2H); ¹³C (75 MHz, CD₃CN): δ 159.0, 157.0, 155.7, 155.5, 154.4, 154.3, 144.7, 143.9, 134.8, 130.8, 129.4, 128.7, 128.5, 127.6, 125.1, 64.0; IR (ATR): ν_{max}/cm^{-1} 3418 (br), 3063 (w), 2939 (w), 2865 (w), 1606 (s), 1548 (m), 1474 (m), 1403 (m), 1241 (m), 1105 (m), 1052 (m), 836 (s) (PF₆); HRMS (ESI) m/z : $[(M - PF_6)]^+$ calcd for $C_{37}H_{28}F_{12}IrN_6OP_2^+$, 1055.1237; found, 1055.1226; MS (ESI) m/z : $[(M - PF_6)]^+$, 1055.21.

Ru(II)–cyt *c* bioconjugate

A solution of Ru(II) **4** (0.9 mg, 975 nmol) in acetonitrile (600 μ L) was added to a solution of 94 mM sodium dihydrogen phosphate, 94 mM ethylenediaminetetraacetic acid, pH 7.0

(3.19 mL) in water (10.9 mL) at room temperature. Purified, reduced iso-1 cytochrome *c* (150 nmol) and tris(2-carboxyethyl)-phosphine (75 nmol) was then added, and the reaction mixture left to stir in the dark for 19 h before concentration, dialysed into water and purified *via* immobilised metal affinity chromatography (IMAC, Ni²⁺) using a gradient from 0 to 125 mM imidazole in sodium dihydrogen phosphate (20 mM), sodium chloride (0.5 M), pH 7.0 in 3.2 mL at 0.5 mL min⁻¹. Fractions containing product were pooled, concentrated, and dialysed into water to yield bioconjugate Ru(II)–cyt *c* (40.1 nmol, 27%). MS (MALDI) m/z : 13 556 $[(M - 2Cl)]^+$, requires 13 559.

Ir(III)–cyt *c* bioconjugate

A solution of Ir(III) **4** (1.04 mg, 1000 nmol) in water (7.86 mL) was added to a solution of 94 mM sodium dihydrogen phosphate, 94 mM ethylenediaminetetraacetic acid, pH 7.0 (2.13 mL) at room temperature. Purified, reduced iso-1 cytochrome *c* (100 nmol) and tris(2-carboxyethyl)phosphine (50 nmol) was then added, and the reaction mixture left to stir in the dark for 23 h before being concentrated, dialysed into water, and purified using the IMAC procedure applied to Ru(II)–cyt *c*. Two separate fractions containing product were concentrated and dialysed into water to yield bioconjugate Ir(III)–cyt *c* (33.0 nmol, 33%). MS (MALDI) m/z : 13 658 $[(M - 2Cl)]^+$, requires 13 650; 13 422 $[(M - 2Cl - tpy)]^+$ requires 13 417; 13 230 $[(M - 2Cl - tpy - Ir)]^+$ requires 13 225.

Enzyme induced polymersomes

In a typical experiment, a 1 mg mL⁻¹ solution of PS₁₄₀-*b*-PAA₄₈ in tetrahydrofuran (33 μ L) was injected into an enzyme/bioconjugate solution (7.5 μ M, 200 μ L) in phosphate buffered saline (150 mM, pH 7.2). The solution was allowed to equilibrate for at least 24 h and extensively dialysed against water using a 50 kDa molecular weight cut-off membrane over 24 h to remove non-encapsulated enzymes.

Photo-induced electron transfer studies

Room temperature photo-induced electron transfer measurements of a non-covalent mixture of Ru(II) **5** and cytochrome *c* and bioconjugate were conducted in specialised small volume quartz cuvettes designed for protein samples, allowing complete exposure to irradiation with a constant area for all experiments (1.0 cm \times 0.3 cm). A solution (80 μ L or 120 μ L) of 5 mM sodium dihydrogen phosphate buffer, 5 mM ethylenediaminetetraacetic acid, pH 7.0 was prepared containing either a 1 : 1 mixture of cytochrome *c* (2.3 μ M) and Ru(II) **5** (2.3 \pm 0.1 μ M) or bioconjugate (2.3 μ M) in bulk or membrane encapsulated samples. Prior to irradiation, cuvettes were degassed for 30 min at 0 °C under reduced pressure (120 mbar) and overlaid with nitrogen in the dark. Samples were irradiated in a nitrogen purged UV-Vis spectrometer with a 465 nm or 372 nm light (LED) source for Ru(II) or Ir(III) bioconjugates, respectively. The LED was placed 2.5 cm from sample and cytochrome *c* reduction was monitored by UV absorbance at 550 nm.

Stern–Volmer studies

Fluorescence emission measurements were made in specialised small volume quartz cuvettes designed for protein samples. Fluorescence measurements were conducted in a mixture of Ir(III) 6 (5 μM) with iso-1 cytochrome *c* (0 to 50 μM) in an aqueous potassium nitrate solution (0.1 M) to maintain constant ionic strength in a total volume of 130 μL . Measurements were performed at 25 and 35 $^{\circ}\text{C}$.

Acknowledgements

We thank the Mark Wainwright Analytical Centre (The University of New South Wales) for providing access to instruments. We thank the Australian Synchrotron Facility for access to the beamline. This work was supported by the Australian Research Council Discovery Project Grants (DP0666325 and DP120101604) and a Future Fellowship to PT (FT120100101). We would also like to thank the UNSW for a scholarship to DH.

Notes and references

- G. T. Hermanson, *Bioconjugate Techniques*, Elsevier Inc., San Diego, CA, 2nd edn, 2008.
- J. Wang, *Chem. Rev.*, 2008, **108**, 814.
- I. Willner, *Science*, 2002, **298**, 2407.
- I. Willner, Y.-M. Yan, B. Willner and R. Tel-Vered, *Fuel Cells*, 2009, **9**, 7.
- K. Ulbrich, J. Strohalm, V. Subr, D. Plocova, R. Duncan and B. Rihova, *Macromol. Symp.*, 1996, **103**, 177.
- J. R. Peterson, T. A. Smith and P. Thordarson, *Chem. Commun.*, 2007, 1899.
- J. R. Peterson, T. A. Smith and P. Thordarson, *Org. Biomol. Chem.*, 2010, **8**, 151.
- J. P. Sauvage, J. P. Collin, J. C. Chambron, S. Guillerez, C. Coudret, V. Balzani, F. Barigelletti, L. De Cola and L. Flamigni, *Chem. Rev.*, 1994, **94**, 993.
- S. Mayo, W. Ellis, R. Crutchley and H. Gray, *Science*, 1986, **233**, 948.
- F. Millett and B. Durham, *Methods Enzymol.*, 2009, **456**, 95.
- M. Heller and U. S. Schubert, *Eur. J. Org. Chem.*, 2003, 947.
- D. C. Goldstein, Y. Y. Cheng, T. W. Schmidt, M. Bhadbhade and P. Thordarson, *Dalton Trans.*, 2011, **40**, 2053.
- X.-J. Yang, F. Drepper, B. Wu, W.-H. Sun, W. Haehnel and C. Janiak, *Dalton Trans.*, 2005, 256.
- S. Hahm, B. Durham and F. Millett, *Biochemistry*, 1992, **31**, 3472.
- K. Wang, H. Mei, L. Geren, M. A. Miller, A. Saunders, X. Wang, J. L. Waldner, G. J. Pielak, B. Durham and F. Millett, *Biochemistry*, 1996, **35**, 15107.
- I. Hamachi, T. Matsugi, S. Tanaka and S. Shinkai, *Bull. Chem. Soc. Jpn.*, 1996, **69**, 1657.
- H. Hofmeier, P. R. Andres, R. Hoogenboom, E. Herdtweck and U. S. Schubert, *Aust. J. Chem.*, 2004, **57**, 419.
- J.-P. Collin, I. M. Dixon, J.-P. Sauvage, J. A. G. Williams, F. Barigelletti and L. Flamigni, *J. Am. Chem. Soc.*, 1999, **121**, 5009.
- M. Maestri, N. Armaroli, V. Balzani, E. C. Constable and A. M. W. C. Thompson, *Inorg. Chem.*, 1995, **34**, 2759.
- H. Hofmeier and U. S. Schubert, *Chem. Soc. Rev.*, 2004, **33**, 373.
- J. Hovinen, *Bioconjugate Chem.*, 2007, **18**, 597.
- K. Lashgari, M. Kritikos, R. Norrestam and T. Norrby, *Acta Crystallogr., Sect. C: Cryst. Struct. Commun.*, 1999, **55**, 64.
- E. C. Constable, J. Lewis, M. C. Liptrot and P. R. Raithby, *Inorg. Chim. Acta*, 1990, **178**, 47.
- D. Keilin, *Proc. R. Soc. London, Ser. B*, 1930, **106**, 418.
- D. E. Shafer, J. K. Inman and A. Lees, *Anal. Biochem.*, 2000, **282**, 161.
- I. Sánchez-Barragán, J. M. Costa-Fernández, A. Sanz-Medel, M. Valledor and J. C. Campo, *Trends Anal. Chem.*, 2006, **25**, 958.
- J. R. Lakowicz, *Principles of Fluorescence Spectroscopy*, Kluwer Academic/Plenum Press, New York, 2nd edn, 1999.
- P. Thordarson, *Chem. Soc. Rev.*, 2011, **40**, 1305.
- W. Leslie, A. S. Batsanov, J. A. K. Howard and J. A. Gareth Williams, *Dalton Trans.*, 2004, 623.
- D. Hvasanov, J. Wiedenmann, F. Braet and P. Thordarson, *Chem. Commun.*, 2011, **47**, 6314.
- R. A. Marcus and N. Sutin, *Biochim. Biophys. Acta*, 1985, **811**, 265.
- H. B. Gray and J. R. Winkler, *Annu. Rev. Biochem.*, 1996, **65**, 537.
- N. S. Hush, *Trans. Faraday Soc.*, 1961, **57**, 557.
- M. Cordes and B. Giese, *Chem. Soc. Rev.*, 2009, **38**, 892.
- J. R. Winkler, T. L. Netzel, C. Creutz and N. Sutin, *J. Am. Chem. Soc.*, 1987, **109**, 2381.
- G. Steinberg-Yfrach, P. A. Liddell, S.-C. Hung, A. L. Moore, D. Gust and T. A. Moore, *Nature*, 1997, **385**, 239.
- G. Steinberg-Yfrach, J.-L. Rigaud, E. N. Durantini, A. L. Moore, D. Gust and T. A. Moore, *Nature*, 1998, **392**, 479.
- H.-J. Choi and C. D. Montemagno, *Nano Lett.*, 2005, **5**, 2538.
- J. R. Peterson and P. Thordarson, *Chiang Mai J. Sci.*, 2009, **26**, 236.
- Bruker, *APEX2 Suite*, Bruker AXS Inc., Madison, WI, USA, 2007.
- G. Sheldrick, *Acta Crystallogr., Sect. A: Foundam. Crystallogr.*, 2008, **64**, 112.
- W. Kabsch, *J. Appl. Crystallogr.*, 1993, **26**, 795.
- A. Winter, C. Ulbricht, E. Holder, N. Risch and U. S. Schubert, *Aust. J. Chem.*, 2006, **59**, 773.